



Numerical study on control strategy of a single cell proton conducting solid oxide fuel cell

Arkadiusz Szczęśniak^{1*}✉

¹Warsaw University, Faculty of Power and Aeronautical Engineering, Institute of Heat Engineering, 21 Nowowiejska Street, 00-665 Warsaw, Poland

✉ arkadiusz.szczesniak@pw.edu.pl

Abstract

The aim of the paper is to examine a control strategy for a single proton conducting solid oxide fuel cell (H+SOFC). The study is based on a dynamic model originating from the steady state reduced order model of H+SOFC. The proposed control strategy is based on a singular PID controller that controls the amount of air delivered to the cathode side of the fuel cell. Additionally, fuel mass flow is correlated with current density to achieve a fixed fuel utilization factor. The concept was tested on typical operating scenarios such as load-follow mode. The study revealed that the singular PID controller is reliable and ensures a safe H+SOFC operation.

Keywords: H+SOFC, control strategy, numerical simulations

Introduction

Fuel cells, in particular, high-temperature Solid Oxide Fuel Cells (SOFC) and Molten Carbonate Fuel Cells are considered as the most promising sources of electricity in the future [1]. This is related to their potentially very high efficiency resulting from the direct conversion of fuel chemical energy into electricity, without using the heat cycle, and possibilities of use in Carbon Capture and Storage (CCS) systems [2–4]. The high operating temperature of SOFCs (700 to 900°C) has serious demerits in terms of overall performance and durability [5,6]. One major flaw is the capital investment cost, as the materials used to manufacture solid oxide fuel cells require high thermal resistance and durability [7]. Reliability and durability are key criteria for systems to gain market acceptance and

establish a positive reputation. With this in mind, proton-conducting SOFCs were proposed, as they have a lower activation energy of proton transport [8]. Proton conductors are also expected to open the way to SOFCs being run at low to intermediate temperature ranges [9]. A key advantage of H+SOFC over standard oxygen ions conducting SOFC is 100% utilization of fuel; thus, there are no anode recirculation solutions needed [10]. However, H+SOFCs require pure hydrogen to the exclusion of other more readily available fuels [11], but they can work in fully reversible mode [12].

This study is focused on examining the H+SOFC control strategies. One of the primary methodologies for the development of a control strategy is mathematical modeling, where dynamic models such as those reported by various researchers [13,14] are used not only for developing a control strategy but also for the analysis of system behavior in emergency conditions [15]. Dynamic models of H+SOFC systems were not scrutinized in the available literature, only SOFC systems and their control strategies were widely studied.

Chen et al. [16] proposed a control strategy for the SOFC-GT hybrid system with anode and cathode recirculation loops. The performance of this control system was evaluated against a control system that did not have a loop for regulating anode temperature during load following. Research has revealed that a designed control system for the hybrid system is feasible and effective.

Lee et al. examined a start-up behavior of SOFC – engine hybrid system [17]. Authors developed individual models of each component and then assembled it into an integrated system model. The dynamic behavior of the system was analyzed at each

stage throughout the entire start-up process from ambient to high operating temperature.

The load following operation of SOFC system integrated with Gas Turbine was examined by Wang [18]. Authors developed a control strategy based on the multi-control loops with the coordinated protection loops. The analysis has shown that the strategy eliminates the instability of SOFC-GT, reduces the SOFC current overshoot by 10.8% during the load step-down operation, and reduces the temperature overshoot by 1.16% in the load step-up operation.

In the available literature, there are numerous studies on the dynamics of SOFC and its control strategies. The comprehensive review of state-of-the-art control strategies of SOFC systems are described by Yang et al. [19]. The authors distinguished eight categories of control strategies: PID, APC, MPC, FLC, FTC, intelligent, and observer-based control. They have indicated that the PID controllers have the simplest structure with relatively high reliability. The H+SOFC control strategy was not discussed in the available literature. The only off-design characteristics with marked optimum zones of operation were introduced by Milewski et al. [20]. Therefore, this study aims to evaluate the PID control strategies for H+SOFC, as this strategy is recognized as reliable and the most widely used SOFC systems. In addition, the Yang et al. [19] noted the more advanced control methods are complicated and therefore there are difficult in application in practical engineering.

Model development

The mathematical model of H+SOFC for steady-state calculations was introduced in the previous paper [21], and the methodology of the model implementation was reported in [22]. The model is based on the reduced order methodology, which is an alternative methodology for fuel cell modeling. A detailed discussion on available models of H+SOFC is reported in the paper by Milewski [24]. Thus, in this section, the only dynamic-oriented relationships are introduced and discussed.

The model describes the H+SOFC examined by Zhu et al. [25], where the single cell with a configuration of NiO+BZCY/BZCY/SSNS was examined. The thicknesses of the BZCY electrolyte layer and the SSNS cathode layer were approximately 46 and 60 mm, respectively. SEM image of the cell is shown in Figure 1. The I-V curve of examined cell is shown in Figure 2.

The previous study revealed that the electrochemical processes and pressure changes are very rapid with respect to thermal dynamic response [13]. Therefore, the presented study is focused mainly on the examination of the thermal dynamic response of the H+SOFC.

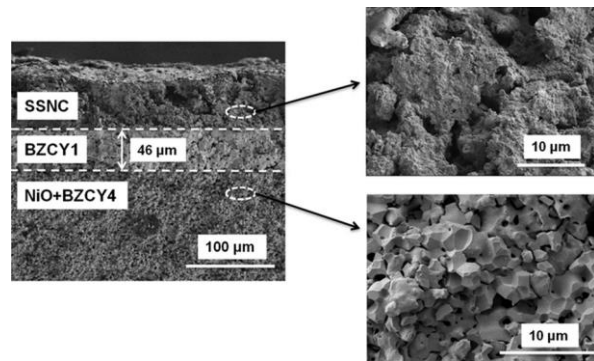


Figure 1: SEM image of a cross-section cell by Zhu et al. [25]

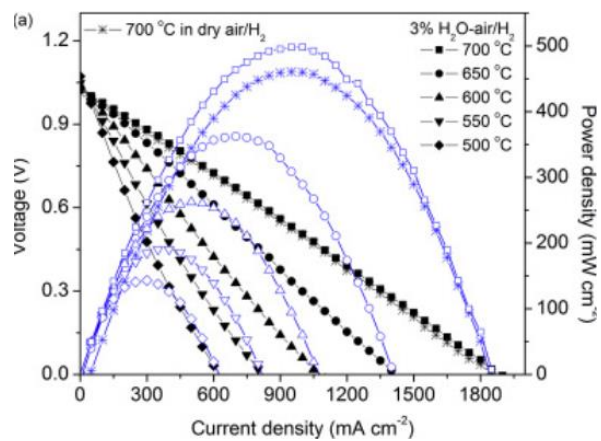


Figure 2: Polarization curves by Zhu et al. [25]

The fuel cell is equipped with two inlet streams and two outlet streams and can be reduced to an OD model. This is the simplest approach but generates a model of the same class as models of other equipment compressors, pumps, and heat exchangers used for system analysis [26]. The set of equations for the OD model is as follows:



$$\begin{cases} \frac{dT_{cell}}{dt} = \frac{\dot{Q}_o + \dot{Q}_{f,c} - 2 \cdot \dot{Q}_{sur} - P_{SOFC} + Q_{f,HH}}{2 \cdot C_{man} + C_f + C_o + C_{cell}} \\ \frac{dp_{cat,out}}{dt} = \frac{(\dot{m}_{cat,in} - \dot{m}_{cat,out}) \cdot R_o \cdot T_{cell}}{V_{cat}} \\ \frac{dp_{an,out}}{dt} = \frac{(\dot{m}_{an,in} - \dot{m}_{an,out}) \cdot R_f \cdot T_{cell}}{V_a} \end{cases} \quad (1)$$

$$\dot{Q}_o = \dot{m}_o \cdot c_{p,o} \cdot (T_{cat,in} - T_{cell}) \quad (2)$$

$$\dot{Q}_{f,c} = \dot{m}_f \cdot c_{p,f} \cdot (T_{an,in} - T_{cell}) \quad (3)$$

$$\dot{Q}_{sur} = k_{sur} \cdot A_{cell} \cdot (T_{cell} - T_{sur}) \quad (4)$$

$$P_{SOFC} = E_{SOFC} \cdot I_{SOFC} \quad (5)$$

$$\dot{Q}_{f,HHV} = \dot{m}_f \cdot HHV_f \cdot \eta_f \quad (6)$$

$$C_{man} = m_{man} \cdot c_{p,man} \quad (7)$$

$$C_{cell} = m_{cell} \cdot c_{p,cell} \quad (8)$$

The parameters used in the equations are listed in Table 1.

Table 1 Main parameters used for the study

Parameter	Value
Specific heat of oxidant, $C_{p,Oxidant}$, kJ/kg/K	1.156
Specific heat of fuel, $C_{p,Fuel}$, kJ/kg/K	15.25
Heat transfer coefficient to surrounding, $k_{Surrounding}$, W/m ² /K	0.1
Higher Heating Value of fuel, HHV_{Fuel} , MJ/kg	144
Specific heat of inter-connector material, $C_{p,Manifold}$, kJ/kg/K	0.5
Specific heat of fuel cell, $C_{p,Cell}$, kJ/kg/K	0.5
Inter-connector weight in relation to fuel cell area, kg/m ²	20.3
Fuel cell weight in relation to fuel cell area, kg/m ²	6

The manifolds at which the H+SOFC is placed have a thickness of 3 mm, which results in a material volume

of 7.5 cm³. Assuming the manifold is made of LaCrO₃, each of them weighs 50 grams. This weight includes additional components, such as manifolds, which deliver the working fluids depending on the specific design of the stack. For this study, it was assumed that the weight of the manifolds in relation to the fuel cell area is 2.03 g/cm². It is important to note that the typical thickness for interconnectors is around 1 mm, and they are often made from stainless steel instead of ceramic materials.

The velocities of working fluids within the channels are influenced by the channel dimensions and the amount of supplied gas. In order to ensure sufficient time for reactions and mixing of reactants, the working fluid velocities should be kept relatively low. According to calculations by the author of this study, the nominal velocities of working fluids are typically less than 5 m/s, with an average velocity of around 1.6 m/s. Because of these low velocities, the pressure drops along the channels can be neglected.

Control strategy of the single cell H+SOFC

In the previous study [27], the key parameters influencing the H+SOFC operation were identified and discussed. During the fuel cell operation the following parameters are used to control the fuel cell operation:

1. Temperature of inlet air and fuel,
2. Volumetric flow of inlet air and fuel,
3. The electric current drawn from the H+SOFC,

The amounts of air and fuel supplied to the fuel cell should enable its proper operation, especially the behavior of the quantities of both fuel utilization and oxidant utilization. In addition, changes in certain parameters interact in a similar way: maintaining the desired temperature of fuel cells can be achieved by either reducing or increasing the amount of air and its temperature since fluid temperature variation is constrained by thermal stress issues. Both of these parameters are related to each other (you cannot cool the fuel cell with overly of hot air, regardless of the amount). Selection of the optimal control strategy in this case is a key issue.

In this study, the design point parameters were adopted from the experiment by Zhu et al. [25] (see Table 2).

Table 2 Nominal operating point of H+SOFC

Parameter	Value
Efficiency, %	45
Specific power, W/cm ²	0.47
Temperature, °C	705
Cell voltage, V	0.565
Current density, A/cm ²	0.83

The singular PID controller is selected to maintain the fuel cell temperature at the set point. This controller regulates the mass flow of inlet air. Optimal PID settings can be determined based on the system's step response to a change in an input parameter. The optimal parameters of PID controller are listed in Table 3.

Table 3 PID settings

Parameter	Value
P	3.264
I	1.6
D	0.5

Results

The H+SOFC was subjected to various disturbances, which could occur during the normal operation. As the fuel cell temperature is the most important parameter, it is kept constant. The temperature is controlled by an inlet air mass flow, which is regulated by a valve equipped with a PID regulator. The singular PID controller is chosen to keep the fuel cell temperature at set point. The PID controls inlet air mass flow.

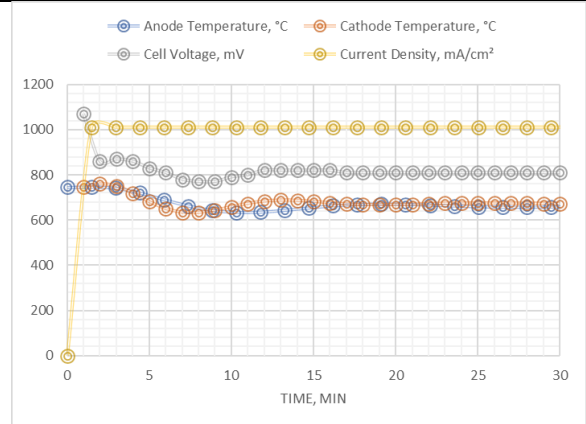


Figure 3: System response to a step change of current drawn from the cell

In the first scenario, the response of the control system to the start of cell operation, i.e. rapid loading of H+SOFC, was tested. It can be seen in Figure 3 that the current drawn caused a temperature increase on the anode and cathode side. The control system compensated the flow, and after about 15 min, the system stabilized all parameters.

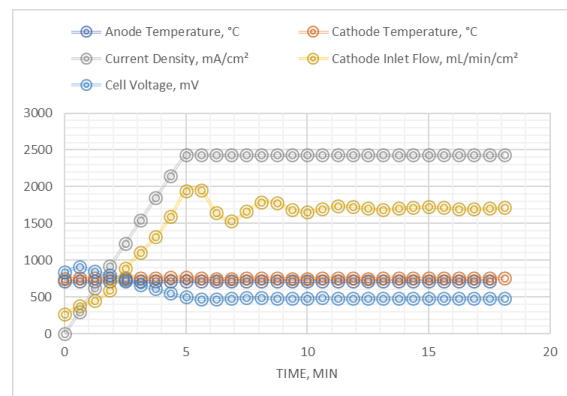


Figure 4: System response to increase of current drawn in 5 minutes

The behavior of the proposed control system was then tested for slow loading of the H+SOFC, i.e. load increase in 5 min (Figure 4). From the time course of the parameters, it can be seen that the control system increased the flow of coolant (oxidant), which resulted in a stabilization of the parameters after about 5 min of changing the operating point.

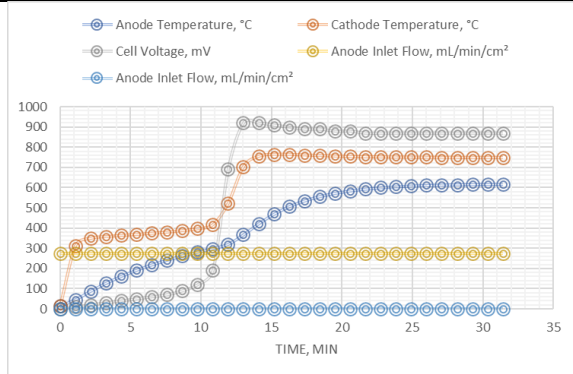


Figure 5: System response to change of point of operation

The next scenario analyzed was to change the operating point, i.e., starting at the idle point (see Figure 5). When current is drawn from H+SOFC, heat is also generated; thus changing the operating point means that not only the current and voltage change but also the temperature of the H+SOFC.

Figure 6 and Figure 7 show the behavior of the fuel cell with and without the proposed control system. From the results shown in Figure 6, it should be noted that, in the absence of the control system, the fuel cell generates a large amount of heat when the operating point is changed (increasing the load), which can cause the fuel cell to overheat and consequently fail.

The control system compensates for the temperature rise by changing the coolant flow. However, due to the temperature dependence of the voltage, it should be noted that the voltage in the fuel cell with the control system stabilizes after 25 min (compared to 5 min). This is due to the control system compensating for the temperature rise caused by the increase in load.

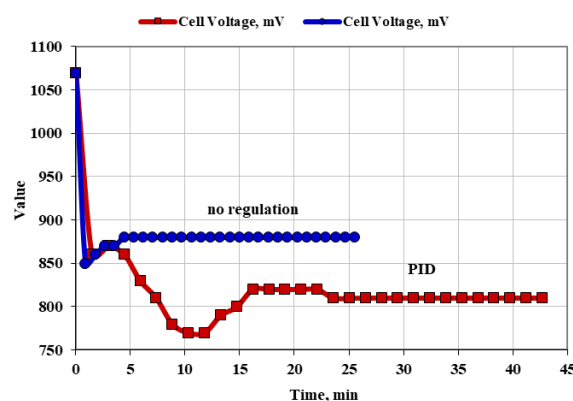


Figure 6: System response to change of point of operation

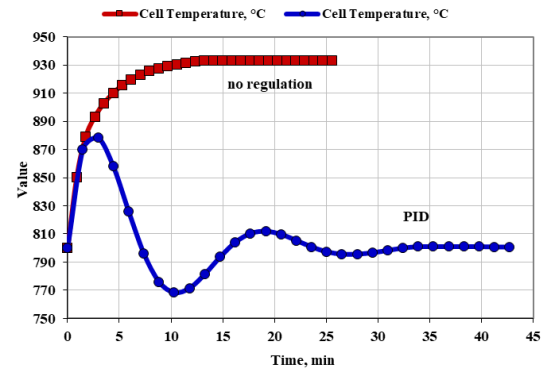


Figure 7: System response to change of point of operation

Discussion and conclusions

The control strategy for a singular H+SOFC is proposed and tested on various scenarios.

The H+SOFC power is directly linked to the release of significant amounts of heat, where the amount of heat results from the subtraction of electrochemical energy from the enthalpy change of the overall reaction. This phenomenon is observed in the fuel cell temperature when the operating point is changed. Additionally, the operating temperature was identified as a key fuel cell operating parameter, which directly influences the electrochemical reaction, which finally affects the H+SOFC power.

Load-follow operation mode showed that the H+SOFC quickly responded with electrochemical reactions, while the thermal response was slower. Thus, the control strategy is oriented toward adjusting the oxidant flow rate to control the fuel cell temperature.

The proposed H+SOFC control strategy is based on a singular PID controller that controls the amount of air delivered to the cathode side of the fuel cell. Additionally, fuel mass flow is correlated with current density to achieve a fixed fuel utilization factor. In fact, the efficiency of the singular laboratory scale fuel cell unit is relatively low, as is the fuel utilization factor is low. Based on mathematical modeling, an analysis of the dynamic operation of a singular fuel cell is presented. In all cases, the singular PID controller is able to keep the fuel cell operation within a safe range.

Nomenclature

T_{cell}	fuel cell temperature
H+SOFC	proton conducting solid oxide fuel cell
SOFC	solid oxide fuel cell
t	time
\dot{Q}_o	heat flux
C	heat capacity
p	pressure
\dot{m}_f	mass flow
V	volume channels
R	specific gas constant
C_p	specific heat capacity
k	heat transfer coefficient
HHV	Higher Heating Value
an	anode
cat	cathode
o	oxidant
f	fuel
sur	surrounding
man	manifold

References

- [1] Sazali N, Salleh WNW, Jamaludin AS, Razali MNM. New Perspectives on Fuel Cell Technology: A Brief Review. *Membr* 2020, Vol 10, Page 99 2020;10:99. <https://doi.org/10.3390/MEMBRANES10050099>.
- [2] Campanari S, Manzolini G, Chiesa P. Using MCFC for high efficiency CO₂ capture from natural gas combined cycles: Comparison of internal and external reforming. *Appl Energy* 2013. <https://doi.org/10.1016/j.apenergy.2013.01.045>.
- [3] Mastropasqua L, Pierangelo L, Spinelli M, Romano MC, Campanari S, Consonni S. Molten Carbonate Fuel Cells retrofits for CO₂ capture and enhanced energy production in the steel industry. *Int J Greenh Gas Control* 2019;88:195–208. <https://doi.org/10.1016/j.IJGGC.2019.05.033>.
- [4] Wang F, Deng S, Zhang H, Wang J, Zhao J, Miao H, et al. A comprehensive review on high-temperature fuel cells with carbon capture. *Appl Energy* 2020;275:115342. <https://doi.org/10.1016/j.apenergy.2020.115342>.
- [5] Abdalla AM, Hossain S, Petra PM, Ghasemi M, Azad AK. Achievements and trends of solid oxide fuel cells in clean energy field: a perspective review. *Front Energy* 2018. <https://doi.org/10.1007/s11708-018-0546-2>.
- [6] Singh M, Zappa D, Comini E. Solid oxide fuel cell: Decade of progress, future perspectives and challenges. *Int J Hydrogen Energy* 2021;46:27643–74. <https://doi.org/10.1016/j.IJHYDENE.2021.06.020>.
- [7] Roshandel R, Golzar F, Astaneh M. Technical economic and environmental optimization of combined heat and power systems based on solid oxide fuel cell for a greenhouse case study. *Energy Convers Manag* 2018;164:144–56. <https://doi.org/10.1016/j.enconman.2018.02.023>.
- [8] Danilov NA, Tarutin AP, Lyagaeva JG, Pikalova EY, Murashkina AA, Medvedev DA, et al. Affinity of YBaCo₄O_{7+δ}-based layered cobaltites with protonic conductors of cerate-zirconate family. *Ceram Int* 2017;43:15418–23. <https://doi.org/10.1016/j.CERAMINT.2017.08.083>.
- [9] De Lorenzo G, Fragiaco P. Electrical and thermal analysis of an intermediate temperature IIR-SOFC system fed by biogas. *ENERGY Sci Eng* 2018;6:60–72. <https://doi.org/10.1002/ese3.187>.



- [10] Genc O, Toros S, Timurkutluk B. Geometric optimization of an ejector for a 4~{kW} {SOFC} system with anode off-gas recycle. *Int J Hydrogen Energy* 2018;43:9413–22. <https://doi.org/10.1016/j.ijhydene.2018.03.213>.
- [11] Recalde M, Woudstra T, Aravind P V. Renewed sanitation technology: A highly efficient faecal-sludge gasification{\textendash}solid oxide fuel cell power plant. *Appl Energy* 2018;222:515–29. <https://doi.org/10.1016/j.apenergy.2018.03.175>.
- [12] Perez-Trujillo JP, Elizalde-Blancas F, Pietra M Della, McPhail SJ. A numerical and experimental comparison of a single reversible molten carbonate cell operating in fuel cell mode and electrolysis mode. *Appl Energy* 2018;226:1037–55. <https://doi.org/10.1016/j.apenergy.2018.05.121>.
- [13] Szczęśniak A, Milewski J, Szabłowski Ł, Bujalski W, Dybiński O. Dynamic model of a molten carbonate fuel cell 1 kW stack. *Energy* 2020;200:117442. <https://doi.org/10.1016/j.energy.2020.117442>.
- [14] Szabłowski Ł, Milewski J. Dynamic analysis of compressed air energy storage in the car. *J Power Technol* 2011;91:23–36.
- [15] Szczęśniak A, Milewski J, Szabłowski Ł, Dybiński O, Futyma K. Numerical Analysis of a Molten Carbonate Fuel Cell Stack in Emergency Scenarios. *J Energy Resour Technol Trans ASME* 2020;142. <https://doi.org/10.1115/1.4048058>.
- [16] Chen J, Liang M, Zhang H, Weng S. Study on control strategy for a SOFC-GT hybrid system with anode and cathode recirculation loops. *Int J Hydrogen Energy* 2017;42:29422–32. <https://doi.org/10.1016/j.ijhydene.2017.09.165>.
- [17] Lee D, Quach TQ, Israel TP, Ahn KY, Bae Y, Kim YS. Analysis of start-up behavior based on the dynamic simulation of an SOFC–engine hybrid system. *Energy Convers Manag* 2022;272:116384. <https://doi.org/10.1016/J.ENCONMAN.2022.116384>.
- [18] Wang X, Lv X, Mi X, Spataru C, Weng Y. Coordinated control approach for load following operation of SOFC-GT hybrid system. *Energy* 2022;248:123548. <https://doi.org/10.1016/J.ENERGY.2022.123548>.
- [19] Yang B, Li Y, Li J, Shu H, Zhao X, Ren Y, et al. Comprehensive summary of solid oxide fuel cell control: a state-of-the-art review. *Prot Control Mod Power Syst* 2022;7:36. <https://doi.org/10.1186/s41601-022-00251-0>.
- [20] Milewski J, Szczęśniak A. Off-design operation of a proton conducting solid oxide fuel cell. *Appl Therm Eng* 2022;212:118599. <https://doi.org/10.1016/j.applthermaleng.2022.118599>.
- [21] Milewski J, Szczęśniak A. A reduced order model of proton conducting Solid Oxide Fuel Cell: A proposal. *Energy Convers Manag* 2021;236:114050. <https://doi.org/10.1016/j.enconman.2021.114050>.
- [22] Milewski J, Szczęśniak A, Szabłowski Ł. A proton conducting solid oxide fuel cell—implementation of the reduced order model in available software and verification based on experimental data. *J Power Sources* 2021;502:229948. <https://doi.org/10.1016/j.jpowsour.2021.229948>.
- [23] Milewski J, Szczęśniak A, Szabłowski Ł, Bernat R. Key Parameters of Proton-conducting Solid Oxide Fuel Cells from the Perspective of Coherence with Models. *Fuel Cells* 2020;fuce.201900077. <https://doi.org/10.1002/fuce.201900077>.
- [24] Milewski J, Szczęśniak A, Szabłowski L. A discussion on mathematical models of proton conducting Solid Oxide Fuel Cells. *Int J Hydrogen Energy* 2019;44:10925–32.
- [25] Zhu A, Zhang G, Wan T, Shi T, Wang H, Wu M, et al. Evaluation of SrScO. 175NbO. 025CoO.



- 803-55 perovskite as a cathode for proton-conducting solid oxide fuel cells: The possibility of in situ creating protonic conductivity and electrochemical performance. *Electrochim Acta* 2018;259:559–65.
- [26] Milewski J, Szcz\keśniak A, Lewandowski J. Dynamic characteristics of auxiliary equipment of SOFC/SOEC hydrogen peak power plant. *IERI Procedia* 2014;9:82–7.
- [27] Milewski J, Szablowski Ł, Szcz\keśniak A. Key parameters of proton conducting Solid Oxide Fuel Cells from power plant point of view n.d.:2–4.